Polymer Chemistry

PAPER

View Article Online
View Journal | View Issue

Cite this: *Polym. Chem.*, 2015, **6**, 6689

Branched alkyl ester side chains rendering large polycyclic (3*E*,7*E*)-3,7-bis(2-oxoindolin-3-ylidene)-benzo[1,2-*b*:4,5-*b*′]difuran-2,6(3*H*,7*H*)-dione (IBDF) based donor–acceptor polymers solution-processability for organic thin film transistors†

Yinghui He, Chang Guo, Bin Sun, Jesse Quinn and Yuning Li*

Received 23rd May 2015,
Accepted 2nd August 2015

DOI: 10.1039/c5py00782h

www.rsc.org/polymers

We report the development and use of a new type of branched alkyl ester side chain for donor–acceptor polymers. The synthesis of the branched alkyl ester side chain precursors is simple and the side chain's branching position and branch length can be adjusted conveniently by choosing the readily available starting materials. (3*E*,7*E*)-3,7-bis(2-oxoindolin-3-ylidene)benzo[1,2-*b*:4,5-*b*′]difuran-2,6(3*H*,7*H*)-dione (IBDF) based donor–acceptor polymers were previously found to have poor solubility in common organic solvents. Herein, we used this new type of branched alkyl ester side chain for the copolymers of IBDF and bithiophene and explored how the branch length would impact the microstructure and charge transport properties of these polymers. With an optimal branch length, the polymer demonstrated ambipolar charge transporting characteristics with a high electron mobility of up to 0.35 $cm^2 V^{-1} s^{-1}$ and a hole mobility of up to 0.20 $cm^2 V^{-1} s^{-1}$ in organic thin film transistors (OTFTs), which is comparable to the one with branched alkyl side chains.

Introduction

Conjugated polymer semiconductors have been widely studied for various organic electronic devices due to their solution-processability, mechanical robustness, and low cost.[1–6] In recent years, specific types of conjugated polymers, donor–acceptor (D–A) polymers, have spurred great interest since they demonstrated high performance in organic thin film transistors (OTFTs) and organic photovoltaics (OPVs).[7–12] Two reasons can account for their high performance: (i) the frontier orbital levels of the polymers can be readily tuned by varying the combination of different donors and acceptors, providing a versatile tool to optimize the band structure of the polymer for the OPV application; (ii) the strong interchain D–A interaction will induce ordered chain packing and shorten the π–π stacking distance, facilitating the interchain charge transport, making D–A materials the currently best performing polymer semiconductors for OTFTs.

So far most efforts have been directed to the development of novel building blocks,[13–15] particularly fused ring acceptor building blocks[16] such as diketopyrrolopyrrole (DPP),[17,18] naphthalene diimide (NDI)[19,20] and isoindigo (IID)[21,22] for high mobility D–A polymers for OTFTs. In general, sufficiently long branched alkyl side chains (Scheme 1) are required to offset the strong aggregation tendency of polymer main chains to render these D–A polymers soluble. Mei *et al.* reported a

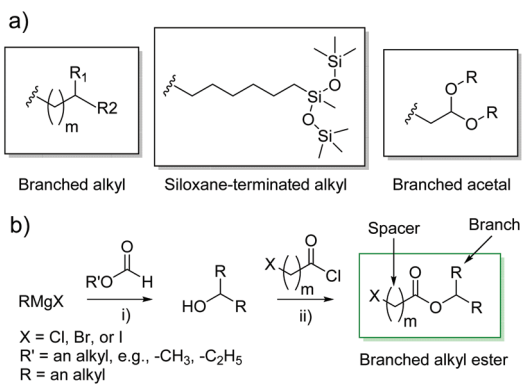

Scheme 1 (a) Side chains used for solubilising D–A polymers. (b) An exemplary synthetic route to the halogenated branched alkyl esters: (i) r.t./ether; (ii) 0 °C/THF.

Department of Chemical Engineering and Waterloo Institute for Nanotechnology (WIN), University of Waterloo, 200 University Avenue West, Waterloo, Ontario N2L 3G1, Canada. E-mail: yuning.li@uwaterloo.ca

†Electronic supplementary information (ESI) available. See DOI: 10.1039/c5py00782h

siloxane-terminated side chain and used it to solubilise an IID polymer, achieving a much improved hole mobility of up to 2.48 $cm^2\ V^{-1}\ s^{-1}$ compared with the alkyl-substituted polymer.[23] We previously found that branched acetal groups (Scheme 1) could be used as solubilising side chains for D–A polymers.[24,25]

Several other studies have shown that engineering of (alkyl) side chains has significant impacts on chain packing, film morphology and hence charge transport properties of polymers.[21,26,27] For example, Lei *et al.* conducted a study on the branching position of the branched alkyl chains on the copolymers of IID and bithiothene (BT).[21] They found that π–π stacking was hindered by the side chains as the spacer group between the IID unit and the branching point of the side chain was CH_2 or C_2H_4 (simply, C1 or C2) (m = 1 or 2 in Scheme 1). When the branching position was moved away further, the backbone became more exposed so that the π–π stacking distance was reduced, which led to improved charge transport properties. The copolymer with a spacer group of C3 (m = 3) achieved the highest OTFT performance. We also found that the side chain length and the branching position greatly influenced the crystallinity, morphology, as well as the π–π stacking distance of a DPP-based polymer, PDQT.[28] By increasing the size of the side chain from 2-octyldodecyl (C20) to 2-decyltetradecyl (C24), the crystallinity of the polymer improved, resulting an increase in mobility from 2.10 $cm^2\ V^{-1}\ s^{-1}$ to 3.37 $cm^2\ V^{-1}\ s^{-1}$. When the distance of the branching point from the backbone was increased from C1 (for 2-octyldodecyl) to C3 (for 4-decylhexadecyl), the π–π distance decreased from 0.386 nm to 0.368 nm, leading to a further improved mobility of up to 6.90 $cm^2\ V^{-1}\ s^{-1}$.

Recently we developed a novel acceptor building block, (3*E*,7*E*)-3,7-bis(2-oxoindolin-3-ylidene)benzo[1,2-*b*:4,5-*b*′]difuran-2,6(3*H*,7*H*)-dione (IBDF in Scheme 2), to construct D–A polymers for OTFTs.[29] The copolymer of C24-substituted IBDF and thiophene, PIBDFT-24, showed a unipolar electron charge transport performance with mobility close to $\sim 10^{-2}\ cm^2\ V^{-1}\ s^{-1}$ in bottom-gate bottom-contact (BGBC) OTFT devices. However, the copolymer based on bithiophene, PIBDFBT-24, is nearly insoluble in any solvent and could not be evaluated in OTFTs due to the very strong intermolecular interaction. Later, Lei *et al.* used a giant 4-octadecyldocosyl (C40) group as the side chain to render the IBDF-BT copolymer, PIBDFBT-40, solution-processable.[30] A high electron mobility of up to 1.74 $cm^2\ V^{-1}\ s^{-1}$ was achieved for this polymer in top-gate bottom-contact (TGBC) devices. (The electron mobility is 0.13 $cm^2\ V^{-1}\ s^{-1}$ in the BGBC devices, somehow lower than in the TGBC devices.) The same group also studied the branching point position of a series of side chains, C38–C43, and found that the side chain (C40) with a C3 spacer gave the best charge transport performance.[26] However, these giant alkyl side chain precursors, alkyl iodide or bromide compounds, are not commercially readily available[31] and the synthesis of these compounds is very tedious,[32] which would limit their use in large-scale applications. We also synthesized **PIBDFBT-40** and found that even with such large side chains this polymer still showed poor solubility in common solvents (*vide infra*). On the other hand, Zhang *et al.* used C24-substituted IBDF and dodecyl-substituted bithiophene unit to improve the solubility of PIBDFBT.[33] However, the polymer exhibited lower OTFT performance (with an electron mobility of ~1 $cm^2\ V^{-1}\ s^{-1}$) in TGBC devices than that of **PIBDFBT-40**, which was probably due to the steric effect introduced by the extra side chains.[34]

Here, we propose to use halogenated branched alkyl ester compounds as precursors to substitute IBDF to form soluble PIBDFBT copolymers. These halogenated branched alkyl esters

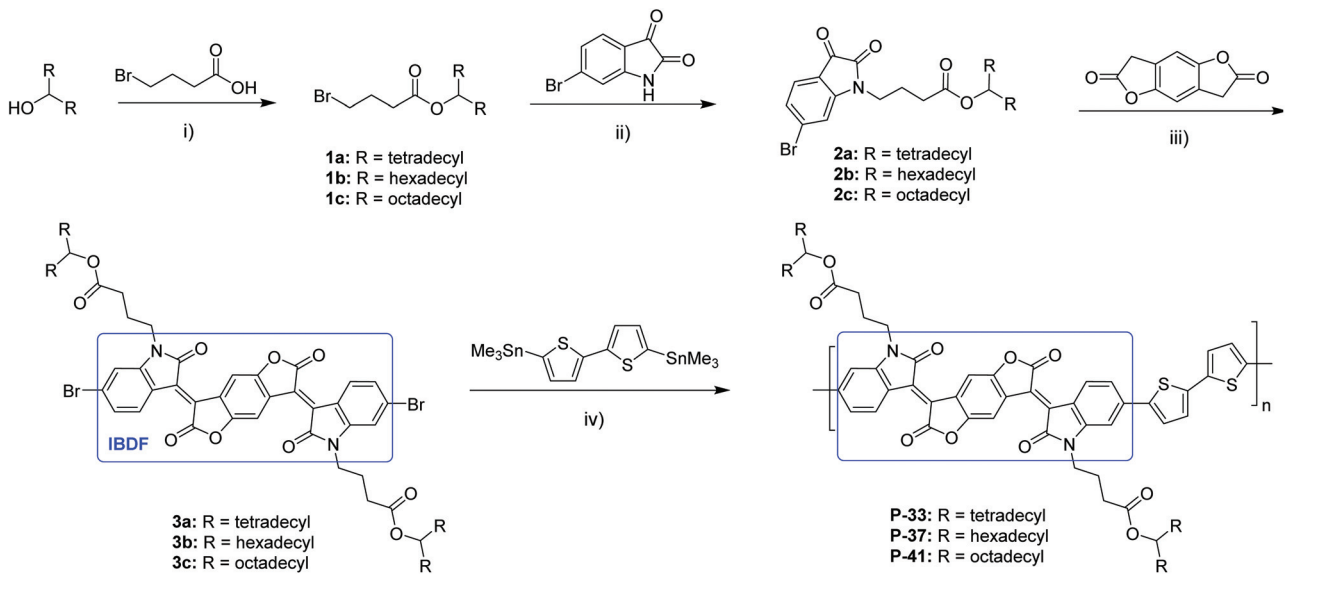

Scheme 2 Synthetic route to branched ester-substituted IBDF polymers **P-33**, **P-37** and **P-41**: (i) $CH_2Cl_2/SOCl_2$/0 °C to r.t., THF/reflux; (ii) DMF/K_2CO_3/50 °C; (iii) AcOH/*p*-toluenesulfonic acid/115 °C; (iv) chlorobenzene/P(*o*-tolyl)$_3$/Pd_2(dba)$_3$/130 °C.

can be conveniently prepared using an exemplary two-step route shown in Scheme 1. The branching point position and the branch length can be varied by using different commercially readily available starting materials. We synthesized three PIBDFBT polymers with these new branched alkyl ester side chains. The polymer with a similar chain length to that of **PIBDFBT-40** exhibited an ambipolar charge transport performance with electron and hole mobilities of up to 0.35 $cm^2 V^{-1} s^{-1}$ and 0.20 $cm^2 V^{-1} s^{-1}$ in BGBC OTFT devices, respectively, which are comparable to those of **PIBDFBT-40**. However, the former showed much improved solubility in common solvents.

Experimental

Materials and characterization

All chemicals were obtained from commercial sources and used as received. Nonacosan-15-ol,[35] tritriacontan-17-ol,[35] heptatriacontan-19-ol,[36] 3,7-dihydrobenzo[1,2-*b*:4,5-*b*′]difuran-2,6-dione[37] and **PIBDFBT-40**[30] were prepared according to the literature methods. High-temperature gel permeation chromatography (HT-GPC) measurements were performed on a Malvern 350 HT-GPC system using 1,2,4-trichlorobenzene as an eluent and polystyrene as standards at a column temperature of 140 °C. Thermogravimetric analysis (TGA) was carried out on a TA Instruments SDT 2960 at a scan rate of 10 °C min^{-1} under nitrogen. The UV-Vis absorption spectra of polymers were recorded on a Thermo Scientific model GENESYS™ 10S VIS spectrophotometer. Cyclic voltammetry (CV) data were obtained on a CHI600E electrochemical analyser using an Ag/AgCl reference electrode and two Pt disk electrodes as the working and counter electrodes in a 0.1 M tetrabutylammonium hexafluorophosphate solution in acetonitrile at a scan rate of 50 mV s^{-1}. Ferrocene was used as the reference, which has a HOMO energy value of −4.8 eV.[38] NMR spectra were recorded with a Bruker DPX 300 MHz spectrometer at room temperature with chemical shifts relative to tetramethylsilane (TMS, 0 ppm). Reflective XRD measurements were carried out on a Bruker D8 Advance diffractometer with Cu Kα radiation (λ = 0.15406 nm) using polymer films spin coated on SiO_2/Si substrates. Atomic force microscopy (AFM) images were taken with a Dimension 3100 scanning probe microscope.

OTFT device fabrication

The bottom-contact bottom-gate (BGBC) configuration was used for all OTFT devices. The preparation procedure of the substrate and device is as follows. A heavily n-doped Si wafer with an ~300 nm-thick SiO_2 layer was patterned with gold source and drain pairs by conventional photolithography and thermal deposition. Then the substrate was treated with air plasma, followed by cleaning with acetone and isopropanol in an ultrasonic bath. Subsequently, the substrate was placed in a 3% dodecyltrichlorosilane (DDTS) solution in toluene at room temperature for 20 min. The substrate was washed with toluene and dried under a nitrogen flow. Then a polymer solution in chloroform (5 mg mL^{-1}) or 1,1,2,2-tetrachloroethane (TCE) (10 mg mL^{-1}) was spin-coated onto the substrate at 3000 rpm for 60 s to give a polymer film (~40 nm), which was further subjected to thermal annealing at different temperatures for 20 min in a glove box. All OTFT devices were characterized in the same glove box using an Agilent B2912A semiconductor analyser. The hole and electron mobilities are calculated in the saturation regime according to the following equation:

$$I_{DS} = \frac{\mu C_i W}{2L}(V_G - V_T)^2$$

where I_{DS} is the drain–source current, μ is the charge carrier mobility, C_i is the gate dielectric layer capacitance per unit area (~11.6 nF cm^{-2}), V_G is the gate voltage, V_T is the threshold voltage, L is the channel length (30 μm), and W is the channel width (1000 μm).

General procedure for the synthesis of brominated branched alkyl esters 1a–1c

To a solution of 4-bromobutyric acid (8.4 g, 50 mmol) in dichloromethane (50 mL) in an ice/water bath, thionyl chloride (8.3 g, 70 mmol) was added. The solution was stirred at room temperature for 4 h. Then the solvent and the excess thionyl chloride were removed under reduced pressure and then the residual was dissolved in tetrahydrofuran (THF) (50 mL). The solution was added dropwise to a suspension of a secondary alcohol (40 mmol) (nonacosan-15-ol for **1a**, tritriacontan-17-ol for **1b**, and heptatriacontan-19-ol for **1c**) in THF (200 mL) at 0 °C. After addition, the reaction mixture was gradually heated to reflux. After 12 h, the reaction mixture was cooled down in an ice/water bath and water was added to quench the reaction. Diethyl ether was added to extract the product. The separated organic phase was washed with saturated $NaHCO_3$ aqueous solution and brine. After removal of the solvent under reduced pressure, the crude product was purified by column chromatography using hexanes/ethyl acetate as the eluent, affording **1** as a white solid.

Nonacosan-15-yl 4-bromobutanoate (1a). Yield: 15.1 g, 66%. ^{1}H-NMR (300 MHz, $CDCl_3$) δ 4.92–4.84 (m, 1H), 3.46 (t, J = 6.4 Hz, 2H), 2.48 (t, J = 7.2 Hz, 2H), 2.22–2.15 (m, 2H), 1.53–1.50 (m, 4H), 1.25 (br, 48H), 0.88 (t, J = 6.6 Hz, 6H).

Tritriacontan-17-yl 4-bromobutanoate (1b). Yield: 21.3 g, 85%. ^{1}H-NMR (300 MHz, $CDCl_3$) δ 4.90–4.84 (m, 1H), 3.46 (t, J = 6.8 Hz, 2H), 2.48 (t, J = 7.0 Hz, 2H), 2.21–2.12 (m, 2H), 1.53–1.45 (m, 4H), 1.25 (br, 56H), 0.88 (t, J = 6.3 Hz, 6H).

Heptatriacontan-19-yl 4-bromobutanoate (1c). Yield: 15.4 g, 56%. ^{1}H-NMR (300 MHz, $CDCl_3$) δ 4.92–4.84 (m, 1H), 3.46 (t, J = 6.4 Hz, 2H), 2.48 (t, J = 7.2 Hz, 2H), 2.22–2.12 (m, 2H), 1.52–1.50 (m, 4H), 1.25 (br, 64H), 0.88 (t, J = 6.8 Hz, 6H).

General procedure for the synthesis of 2a–2c

In a two-neck round bottom flask, 6-bromoisatin (1.13 g, 5 mmol), potassium carbonate (1.38 g, 10 mmol), **1** (5 mmol) and *N*,*N*′-dimethylformamide (DMF) (40 mL) were added. The reaction mixture was then stirred at 50 °C for 18 h. The solvent was removed and the residual was dissolved in dichloro-

methane and washed with water. After removal of the solvent, the crude product was purified by column chromatography using a mixture of hexanes and ethyl acetate as the eluent, affording **2** as an orange solid.

Nonacosan-15-yl 4-(6-bromo-2,3-dioxoindolin-1-yl)butanoate (2a). Yield: 2.55 g, 71%. ^{1}H-NMR (300 MHz, $CDCl_3$) δ 7.46 (d, J = 7.8 Hz, 1H), 7.28 (dd, J = 8.1 Hz, 1.5 Hz, 1H), 7.23 (d, J = 1.5 Hz, 1H), 4.94–4.86 (m, 1H), 3.77 (t, J = 7.5 Hz, 2H), 2.42 (t, J = 6.9 Hz, 2H), 2.05–1.96 (m, 2H), 1.54–1.52 (m, 4H), 1.25 (br, 48H), 0.88 (t, J = 6.6 Hz, 6H).

Tritriacontan-17-yl 4-(6-bromo-2,3-dioxoindolin-1-yl)butanoate (2b). Yield: 2.56 g, 66%. ^{1}H-NMR (300 MHz, $CDCl_3$) δ 7.46 (d, J = 7.8 Hz, 1H), 7.28 (dd, J = 8.1 Hz, 1.4 Hz, 1H), 7.23 (d, J = 1.4 Hz, 1H), 4.94–4.86 (m, 1H), 3.77 (t, J = 7.4 Hz, 2H), 2.42 (t, J = 6.9 Hz, 2H), 2.05–1.95 (m, 2H), 1.55–1.51 (m, 4H), 1.25 (br, 56H), 0.88 (t, J = 6.9 Hz, 6H).

Heptatriacontan-19-yl 4-(6-bromo-2,3-dioxoindolin-1-yl)-butanoate (2c). Yield: 2.45 g, 59%. ^{1}H-NMR (300 MHz, $CDCl_3$) δ 7.46 (d, J = 7.8 Hz, 1H), 7.28 (dd, J = 8.1 Hz, 1.5 Hz, 1H), 7.23 (d, J = 1.5 Hz, 1H), 4.94–4.86 (m, 1H), 3.77 (t, J = 7.4 Hz, 2H), 2.42 (t, J = 6.9 Hz, 2H), 2.05–1.98 (m, 2H), 1.55–1.51 (m, 4H), 1.25 (br, 64H), 0.88 (t, J = 6.9 Hz, 6H).

General procedure for the synthesis of 3a–3c

In a two-neck round bottom flask, **2** (2 mmol), *p*-toluenesulfonic acid (53 mg, 0.28 mmol), 3,7-dihydrobenzo[1,2-*b*:4,5-*b*′]-difuran-2,6-dione (0.19 g, 1 mmol) and acetic acid (10 mL) were added. The reaction mixture was stirred at 115 °C for 24 h. Upon cooling to room temperature, the reaction mixture was filtered and the filter cake was washed with methanol. The crude product was then purified by column chromatography using a mixture of hexanes and chloroform as the eluent, affording **3** as a black solid.

Di(nonacosan-15-yl) 4,4′-((3*E*,3′*E*)-(2,6-dioxobenzo[1,2-*b*:4,5-*b*′]-difuran-3,7(2*H*,6*H*)-diylidene)bis(6-bromo-2-oxoindoline-1-yl-3-ylidene))dibutyrate (3a). Yield: 0.56 g, 35%. ^{1}H-NMR (300 MHz, $CDCl_3$) δ 9.06 (s, 2H), 8.90 (d, J = 8.4 Hz), 7.19 (dd, J = 5.1 Hz, 1.6 Hz, 2H), 7.06 (d, J = 1.5 Hz, 2H), 4.94–4.90 (m, 2H), 3.83 (t, J = 7.2 Hz, 4H), 2.44 (t, J = 6.9 Hz, 4H), 2.05–2.01 (m, 4H), 1.53(br, 4H), 1.23 (br, 96H), 0.87 (t, J = 6.8 Hz, 12H). ^{13}C-NMR (75 MHz, $CDCl_3$) δ 172.57, 167.19, 151.96, 146.76, 135.74, 131.74, 129.47, 127.11, 126.72, 126.07, 126.02, 119.89, 112.10, 112.23, 75.22, 39.76, 34.02, 32.12, 31.60, 29.89, 29.75, 29.57, 25.58, 22.89, 14.30. HR-MS (M^+) calc. for $C_{92}H_{139}O_{10}N_2Br_2$: 1589.88066; found: 1589.87910.

Di(tritriacontan-17-yl) 4,4′-((3*E*,3′*E*)-(2,6-dioxobenzo[1,2-*b*:4,5-*b*′]-difuran-3,7(2*H*,6*H*)-diylidene)bis(6-bromo-2-oxoindoline-1-yl-3-ylidene))dibutyrate (3b). Yield: 0.44 g, 26%. ^{1}H-NMR (300 MHz, $CDCl_3$) δ 9.09 (s, 2H), 8.93 (d, J = 8.7 Hz), 7.22 (dd, J = 5.1 Hz, 1.6 Hz, 2H), 7.08 (d, J = 1.5 Hz, 2H), 4.94–4.90 (m, 2H), 3.84 (t, J = 7.2 Hz, 4H), 2.44 (t, J = 6.9 Hz, 4H), 2.06–2.01 (m, 4H), 1.53(br, 4H), 1.23 (br, 112H), 0.87 (t, J = 6.6 Hz, 12H). ^{13}C-NMR (75 MHz, $CDCl_3$) δ 172.57, 167.19, 151.96, 146.75, 135.74, 131.74, 129.47, 127.01, 126.72, 126.07, 126.02, 119.89, 112.10, 111.20, 75.22, 39.76, 34.26, 32.12, 31.60, 29.89, 29.75, 29.57, 25.58, 22.89, 14.30. HR-MS (M^+) calc. for $C_{100}H_{155}O_{10}N_2Br_2$: 1701.99718; found: 1702.00430.

Di(heptatriacontan-19-yl) 4,4′-((3*E*,3′*E*)-(2,6-dioxobenzo[1,2-*b*:4,5-*b*′]difuran-3,7(2*H*,6*H*)-diylidene)bis(6-bromo-2-oxoindoline-1-yl-3-ylidene))dibutyrate (3c). Yield: 0.44 g, 24%. ^{1}H-NMR (300 MHz, $CDCl_3$) δ 9.10 (s, 2H), 8.94 (d, J = 8.7 Hz, 2H), 7.25 (d, J = 7.8 Hz, 2H), 7.09 (s, 2H), 4.92 (m, 2H), 3.84 (t, J = 6.8 Hz, 4H), 2.44 (t, J = 6.8 Hz, 4H), 2.05–2.03 (m, 4H), 1.51–1.24 (br, 132H), 0.87 (t, J = 6.4 Hz, 12H). ^{13}C-NMR (75 MHz, $CDCl_3$) δ 172.56, 167.19, 151.97, 146.76, 135.77, 131.72, 129.46, 127.03, 126.75, 126.13, 126.01, 119.90, 112.06, 111.19, 75.21, 39.70, 34.26, 32.12, 31.59, 29.90, 29.76, 29.57, 25.57, 22.89, 14.32. HR-MS (M^+) calc. for $C_{108}H_{171}O_{10}N_2Br_2$: 1814.12996; found: 1814.12950.

General procedure for the synthesis of P-33, P-37, and P-41

In a Schlenk flask, **3** (0.0453 mmol), 5,5′-bis(trimethylstannyl)-2,2′-bithiophene (22.6 mg, 0.0453 mmol), tri(*o*-tolyl)phosphine (1.1 mg, 3.6 μmol), tris(dibenzylideneacetone)dipalladium (0.8 mg, 0.9 μmol) and anhydrous chlorobenzene (4 mL) were added under an argon atmosphere. The reaction mixture was then stirred at 130 °C for 48 h. Upon cooling to room temperature, the reaction mixture was poured into methanol and the precipitate was collected by filtration, followed by Soxhlet extraction.

P-33: This polymer was purified by Soxhlet extraction using acetone, hexanes, chloroform and TCE. Yield: 71 mg, 98% (from the TCE fraction).

P-37: This polymer was purified by Soxhlet extraction using acetone, hexanes and chloroform. Yield: 74 mg, 95% (from the chloroform fraction).

P-41: This polymer was purified by Soxhlet extraction using acetone, hexanes and chloroform. Yield: 76 mg, 92% (from the chloroform fraction).

Results and discussion

The synthesis of three PIBDFBT polymers having branched alkyl ester side chains, **P-33**, **P-37** and **P-41**, is outlined in Scheme 2. Previous studies have shown that a spacer C3 is optimal for IID[14] and IBDF[15] based polymers in OTFTs. Hence we used branched alkyl side chains with a C3 spacer and varied the branch length (–$C_{14}H_{29}$, –$C_{16}H_{33}$ and –$C_{18}H_{37}$) to substitute the IBDF unit. Three branched alkyl ester bromides (**1a–c**) were conveniently synthesized by reacting the respective secondary alcohols with 4-bromobutyryl chloride, which was prepared *in situ* by using 4-bromobutyric acid and thionyl chloride. **1a–c** were then reacted with 6-bromoisatin to form the branched alkyl ester-substituted 6-bromoisatins **2a–c**. Condensation of 3,7-dihydrobenzo[1,2-*b*:4,5-*b*′]difuran-2,6-dione with two equivalents of **2a–c** produced the IBDF monomers **3a–c**. Finally three copolymers **P-33**, **P-37**, and **P-41** were synthesized *via* the Stille coupling polymerization following a similar procedure reported previously.[29] The yields for **P-33**, **P-37**, and **P-41** are 98%, 95% and 92%, respectively, after puri-

Table 1 Summary of the properties of polymers

Polymer	Solubility testing[a]	M_n (kDa)	PDI	$\lambda_{max}^{sol/film}$ (nm)	E_g^{opt} (eV)	E_{HOMO}/E_{LUMO} (eV)	E_g^{CV} (eV)
P-33	TCE[b]	16	4.0	847/847	1.29	−5.68/−3.85	1.83
P-37	TCE, CF, CB, DCB,	40	3.4	847/847	1.29	−5.72/−3.87	1.85
P-41	TCE, CF, DCM, CB, DCB, TL, XL	39	4.8	840/840	1.31	−5.73/−3.85	1.88
PIBDFBT-40	TCE, DCB	40	8.4	780/782	1.29	−5.72/−3.88	1.84

[a] Solubility testing was conducted by dissolving the polymer in a solvent (~5 mg mL^{-1}) at room temperature (sometimes with the aid of heating before cooling to room temperature). [b] Solvent in which the polymer can be completely dissolved. TCE: 1,1,2,2-tetrachloroethane; CF: chloroform; DCM: dichloromethane; CB: chlorobenzene; DCB: *o*-dichlorobenzene; TL: toluene; XL: xylene.

fication by Soxhlet extraction. We tested the solubility of the polymers (**P-33**, **P-37**, **P-41** and **PIBDFBT-40**) in various common organic solvents including 1,1,2,2-tetrachloroethane (TCE), chloroform (CF), dichloromethane (DCM), chlorobenzene (CB), *o*-dichlorobenzene (DCB), toluene (TL), and xylene (XL) at room temperature (Table 1). **P-41** with the largest side chains can be easily dissolved in all the above solvents. **P-37** is less soluble than **P-41**, but can still be dissolved in CF, TCE, CB, and DCB. **P-33** with the smallest side chains is only soluble in TCE among the solvents tested. We also tested the solubility of **PIBDFBT-40**, which has branched C40 alkyl side chains. This polymer can only be dissolved in TCE and DCB. Compared to the C40 branched alkyl side chain, the C37 branched alkyl side chain with a similar size appears to have stronger solubilizing ability. High temperature-gel permeation chromatography (HT-GPC) was used to evaluate the molecular weights of these polymers. The column temperature was set at 140 °C and 1,2,4-trichlorobenzene was used as the eluent. **P-33** has a rather low average molecular weight (M_n) of 16 kDa, which is probably due to its poor solubility in the polymerization medium (CB as the solvent). The molecular weights of **P-37** and **P-41** are much higher with an M_n of 40 kDa and 39 kDa, respectively, owing to their better solubility enabled by their larger side chains. **PIBDFBT-40** has a similar M_n of 40 kDa, but the polydispersity (PDI) is extremely large (8.4), which is thought to be caused by the strong polymer chain aggregation or poorer solubility even at such a high temperature (ESI†). The thermal stability of the polymers was characterized by thermogravimetric analysis (TGA, ESI†). The 5% weight loss temperatures ($T_{-5\%}$) are 290 °C, 300 °C and 300 °C for **P-33**, **P-37** and **P-41**, respectively, indicating their quite good thermal stability. However, these polymers started to decompose at lower temperatures compared to that of **PIBDFBT-40** ($T_{-5\%}$ = ~380 °C) probably due to the less thermally stable ester groups.

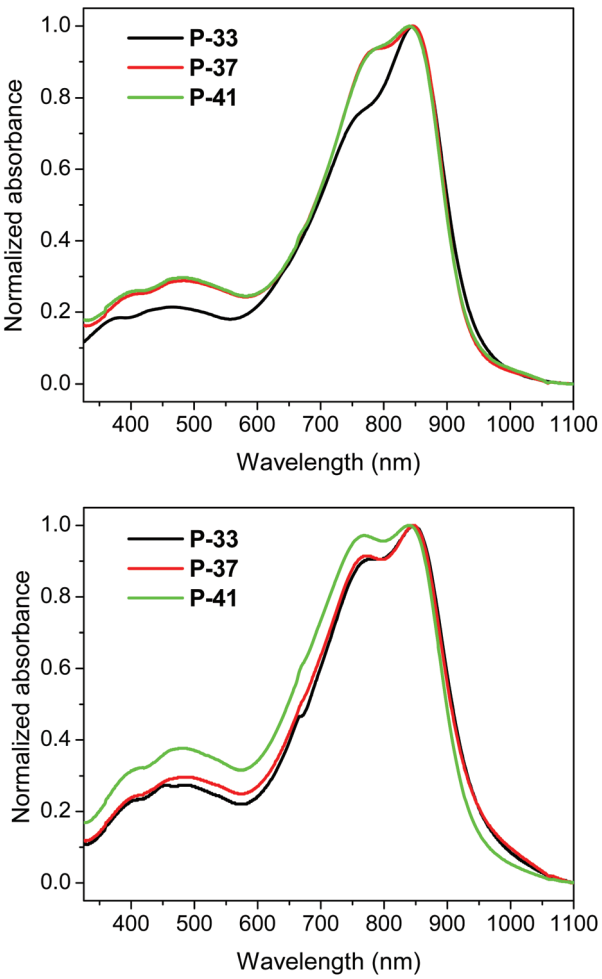

Fig. 1 The UV-Vis absorption spectra in solution (top) and in film (bottom).

The optical properties of the polymers in dilute solutions and thin films are characterized by UV-Vis absorption spectroscopy (Fig. 1 and Table 1). **P-33** and **P-37** showed an identical wavelength of maximum absorption (λ_{max}) at 847 nm in solutions and films. On the other hand, **P-41** showed a λ_{max} at ~840 nm in solution and the solid state, which is blue-shifted compared to those of **P-33** and **P-37**. This implies that the backbone of **P-41** is less coplanar than those of **P-33** and **P-37**, likely caused by the stronger interactions of its larger side chains with solvent molecules in solution and between themselves in the film to make the backbone slightly more twisted.[28,39] All polymers showed vibronic splitting absorption peaks at ~750 nm in both dilute solutions and films. In solution, the vibronic splitting absorption peak (or shoulder) for **P-33** is less pronounced with respect to the peak at λ_{max} compared to the other two polymers, which might be due to its lower molecular weight. In films, the vibronic splitting absorp-

tion peaks for all polymers became more resolved as compared to those in the solution spectra. This could be due to the excitonic–vibronic coupling induced by interchain aggregation in the solid state.[40] The absorption profiles of these alkyl ester substituted polymers are markedly different from those of **PIBDFBT-40** in both solution and film (ESI†). For **PIBDFBT-40**, the λ_{max} was observed at ~780 nm in both solution and film, while only a shoulder at ~840 nm appeared in the film. These results suggest that the ester side chains have an impact on the backbone conjugation. The optical bandgaps (E_g's) were estimated using the onset absorption wavelengths to be ~1.29 eV for **P-33**, **P37** and **PIBDFBT-40** and ~1.31 eV for **P-41**. Cyclic voltammetry (CV) was used to study the electrochemical properties of the polymers (Fig. 2 and Table 1). All polymers showed both the reductive and oxidative peaks. The highest occupied molecular orbital and lowest unoccupied molecular orbital (HOMO and LUMO) levels were estimated using the onset oxidation and reduction potentials. All three polymers have similar HOMO levels (ranging from −5.68 eV to −5.73 eV) and LUMO levels (ranging from −3.85 eV to −3.87 eV). The similar HOMO and LUMO levels of these polymers indicate that side chains have minimal impacts on the electrochemical properties of the polymers. These energy levels are similar to those of **PIBDFBT-40** (E_{HOMO} = −5.72 eV; E_{LUMO} = −3.88 eV). The frontier orbital levels of these polymers fall in the ranges where ambipolar charge transport performance might be observed.[41,42] The band gaps of these polymers determined from the LUMO and HOMO levels obtained by the CV measurements are 1.83–1.88 eV (Table 1), which are much larger than their optical band gaps (1.29–1.31 eV). These discrepancies most likely originated from the exciton binding energy of the conjugated polymers, which can be as high as ~0.4–1 eV.[43,44]

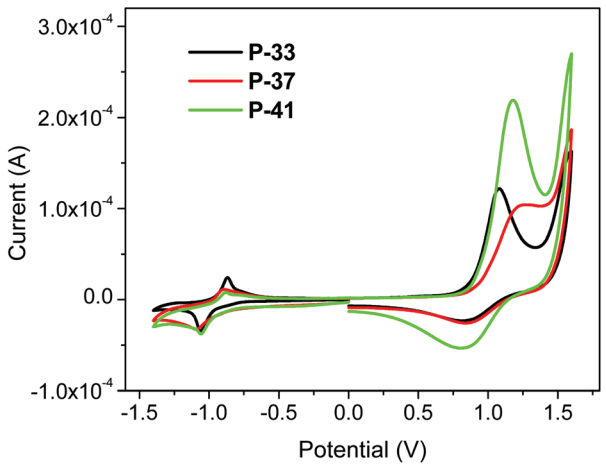

Fig. 2 The cyclic voltammetry (CV) diagrams of **P-33**, **P-37** and **P-41** thin films measured in a 0.1 M tetrabutylammonium hexafluorophosphate solution in anhydrous acetonitrile at a scan rate of 50 mV s^{-1}.

To probe how the length of the alkyl branch (R) would impact the charge transport, these polymers were used as channel semiconductor materials in BGBC OTFT devices using SiO_2/Si wafer as the substrate. All three polymers showed ambipolar charge transporting characteristics with higher electron mobilities than hole mobilities (Table 2). When the annealing temperature was increased from 100 °C to 200 °C, the carrier mobility improved gradually for all devices. However, it was found that further increasing the annealing temperature to 250 °C led to performance degradation. Among three polymers, **P-37** with $C_{16}H_{33}$ as the branch showed the best device performance with the average electron mobility of 0.32 cm^2 V^{-1} s^{-1} and hole mobility of 0.15 cm^2 V^{-1} s^{-1} when the films were annealed at 200 °C (Fig. 3). **P-33** showed the average electron and hole mobilities of 0.10 cm^2 V^{-1} s^{-1} and 0.051 cm^2 V^{-1} s^{-1}, respectively, for the films annealed at 200 °C. The lower performance of **P-33** is considered due to its lower molecular weight as well as its poorer thin film morphology (see below). The best performance for **P-41** was obtained for the films annealed at 200 °C, with an average electron mobility of 0.072 cm^2 V^{-1} s^{-1} and a hole mobility of 0.027 cm^2 V^{-1} s^{-1}. The poorest charge transport performance of **P-41** among three polymers is probably the result of its more twisted backbone as previously discussed on the UV-Vis absorption spectra and its poor film morphology (see below). To compare the ester chains with alkyl side chains, we also tested **PIBDFBT-40** as a channel semiconductor in BGBC devices under the same conditions. Ambipolar charge transport was also observed for the devices based on **PIBDFBT-40** (Table 2). For the devices

Table 2 OTFT device performance of the polymers annealed at different annealing temperatures

Polymer	Annealing temperature (°C)	μ_e (cm^2 V^{-1} s^{-1})		μ_h (cm^2 V^{-1} s^{-1})	
		Avg.	Max.	Avg.	Max.
P-33	100	0.081 ± 0.005	0.089	0.034 ± 0.012	0.050
	150	0.092 ± 0.010	0.11	0.050 ± 0.011	0.065
	200	0.10 ± 0.015	0.12	0.051 ± 0.010	0.065
P-37	100	0.24 ± 0.022	0.28	0.096 ± 0.009	0.11
	150	0.27 ± 0.025	0.30	0.10 ± 0.010	0.12
	200	0.32 ± 0.023	0.35	0.15 ± 0.037	0.20
P-41	100	0.041 ± 0.003	0.045	0.023 ± 0.004	0.028
	150	0.054 ± 0.004	0.058	0.023 ± 0.004	0.029
	200	0.072 ± 0.003	0.074	0.027 ± 0.002	0.030
PIBDFBT-40	200	0.39 ± 0.032	0.43	0.17 ± 0.043	0.24

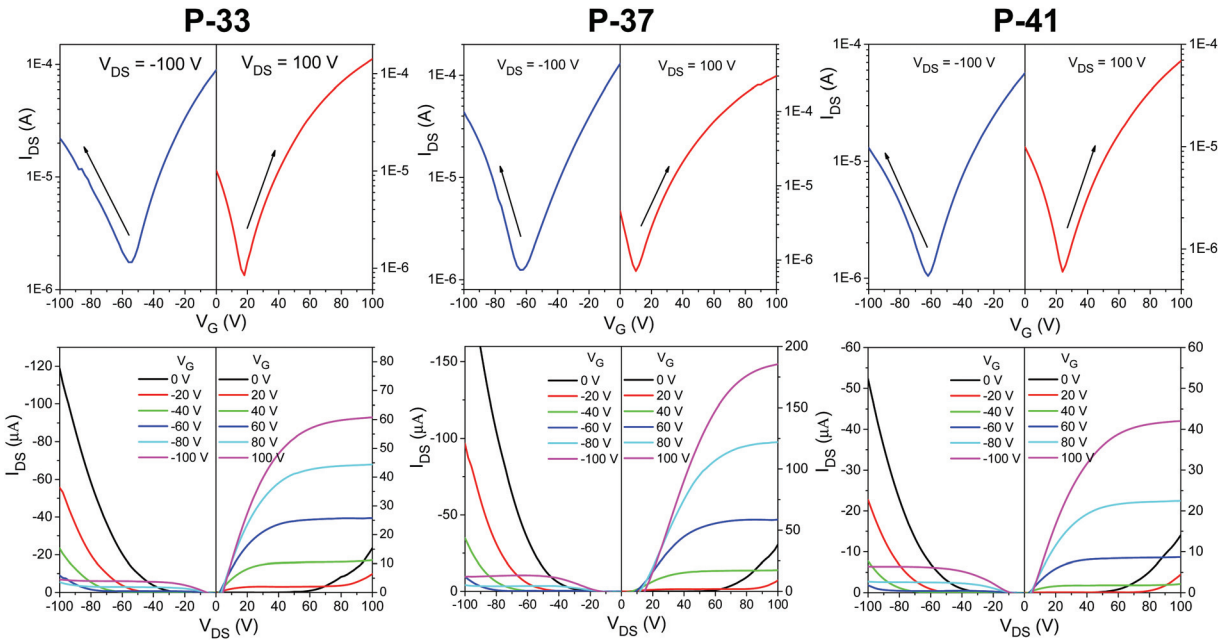

Fig. 3 Transfer (top) and output (bottom) curves of BGBC OTFT devices with 200 °C-annealed **P-33**, **P-37** and **P-41** films. Device dimensions: channel length (L) = 30 μm; channel width (W) = 1000 μm.

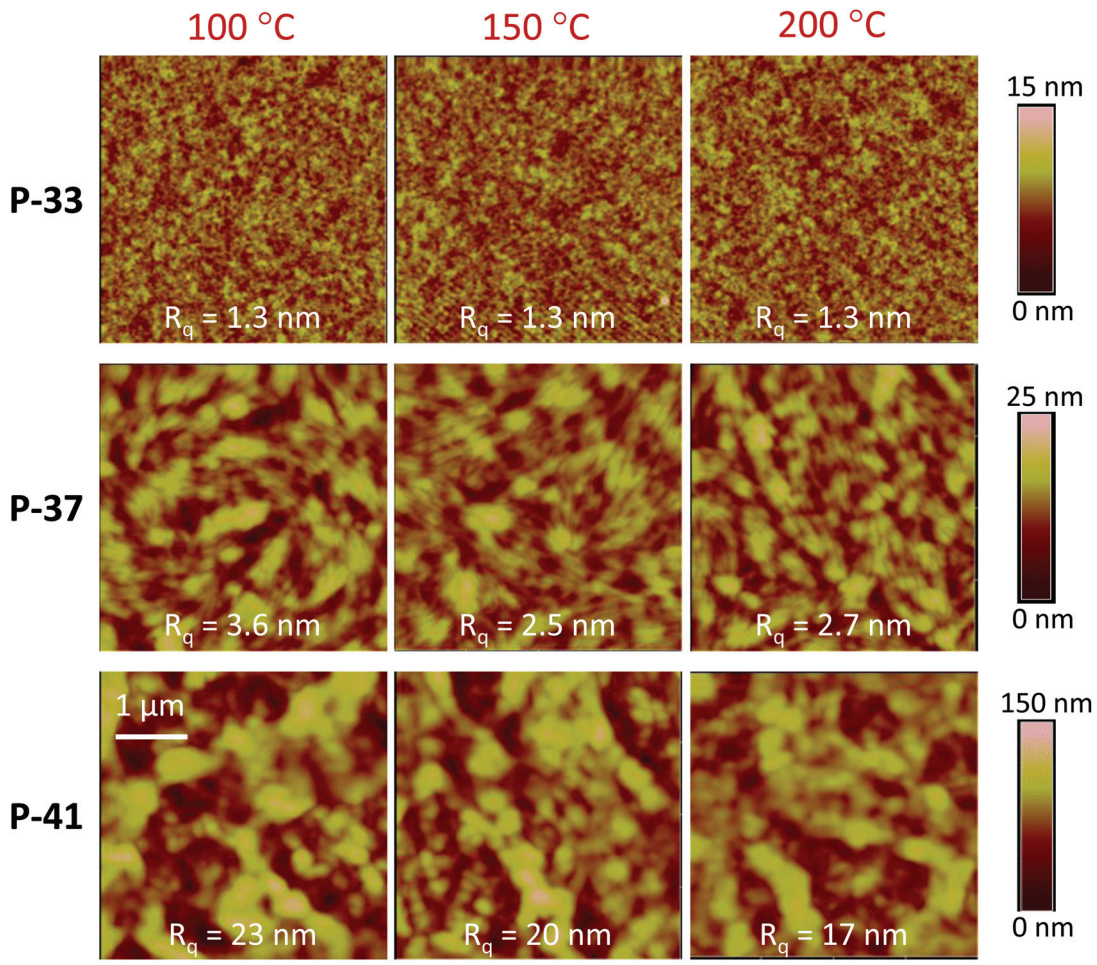

Fig. 4 AFM images (4 μm × 4 μm) of polymer films annealed at different temperatures.

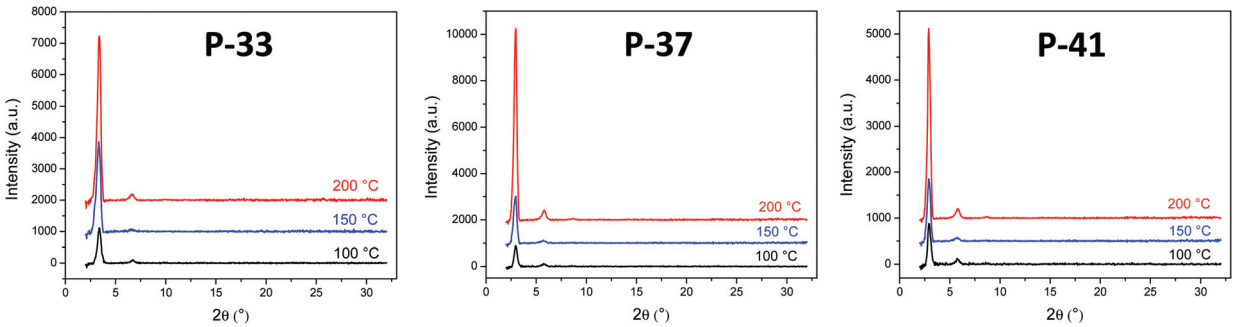

Fig. 5 Reflective XRD patterns of **P-33**, **P-37** and **P-41** films annealed at different temperatures.

annealed at 200 °C, the average electron mobility was 0.39 cm^2 V^{-1} s^{-1} and the average hole mobility was 0.22 cm^2 V^{-1} s^{-1}, which are slightly higher than those of **P-37**. Our results indicate that ester side chains can be used as solubilizing chains for D–A polymers and the resulting polymers can achieve comparable charge transporting properties in OTFTs to those with alkyl side chains.

To further understand why **P-37** showed better charge transport properties than **P-33** and **P-41**, we characterized the microstructures of the polymer thin films with atomic force microscopy (AFM, Fig. 4) and X-ray diffraction (XRD, Fig. 5). The thin film samples were prepared under the same conditions as those used for the OTFT devices. In the AFM images of the **P-33** films, very smooth surfaces with a low root mean squared roughness (R_q) of 1.3 nm were observed. However only small grains with poor interconnections can be seen, which might be due to the low molecular weight of **P-33**. For the **P-37** films, well-interconnected large fibre-like domains are observed, which is regarded to be beneficial for the charge transport.[45] The as-spun **P-41** films showed very large grains and grain boundaries with an R_q of 23 nm. With increasing annealing temperature, the film morphology slightly improved, but the films are still very rough. The very poor film morphology might be another reason for the poor charge transport performance of **P-41**.

Reflective mode XRD was employed to investigate the chain packing of these polymers in spin-coated thin films (Fig. 5). The as-spun **P-33**, **P-37** and **P-41** films showed the primary diffraction peaks at 2θ = 3.37°, 2.97° and 2.90°, which correspond to their inter-lamellar *d*-spacing distances of 2.62 nm, 2.97 nm and 3.04 nm, respectively, agreeing with the increasing size of their side chains. Since there are no diffractions corresponding to the co-facial π–π distance (normally at 2θ = ~20–25°), the polymer chains presumably adopted an edge-on orientation motif with respect to the substrate.[46,47] As the annealing temperature was increased, the intensity of the primary diffraction peaks increased and the secondary diffraction peaks became more visible, indicating that longer range ordering was achieved. This explains why the carrier mobility increased with increasing annealing temperature. The 200 °C-annealed **P-37** film showed the strongest diffraction peaks and thus the most ordered chain packing, which also accounted for its best charge transport performance among three polymers.

Conclusions

In summary, a new type of branched alkyl ester side chain was developed and used for the IBDF-based D–A polymers. Branched alkyl ester bromides, which were used for side chain substitution with various branch lengths, could be conveniently synthesized compared to the long branched alkyl halides. We established a correlation between the size of the alkyl ester side chains and the polymer properties, *e.g.*, solubility, film morphology and charge transport. When the ester side chain is undersized (C33), the polymer P-33 showed poor solubility and processability. Small grains with poor interconnection were present in the polymer thin film, which is detrimental to the inter-grain charge transport. When the ester side chain is oversized (C41), the polymer P-41 has excellent solubility and processability. However, main chain twisting, rough morphology, and poor chain packing have resulted, leading to a low charge transport performance in OTFTs. **P-37** with the ester side chain C37 was found to be optimal for achieving good solubility, good film morphology and high crystallinity. A high electron mobility of up to 0.35 cm^2 V^{-1} s^{-1} and a hole mobility of 0.20 cm^2 V^{-1} s^{-1} were obtained for **P-37** in BGBC OTFTs, which is comparable to the polymer with the same backbone and similarly long branched alkyl side chains. Our results demonstrate that branched alkyl ester side chains are a novel useful type of solubilizing group for conjugated polymers.

Acknowledgements

The authors thank the Natural Sciences and Engineering Research Council (NSERC) of Canada for financial support of this work (Discovery Grants #402566-2011).

Notes and references

1 D. T. McQuade, A. E. Pullen and T. M. Swager, *Chem. Rev.*, 2000, **100**, 2537–2574.
2 Y.-J. Cheng, S.-H. Yang and C.-S. Hsu, *Chem. Rev.*, 2009, **109**, 5868–5923.
3 L. Dai, B. Winkler, L. Dong, L. Tong and A. W. H. Mau, *Adv. Mater.*, 2001, **13**, 915–925.
4 A. Facchetti, *Chem. Mater.*, 2011, **23**, 733–758.
5 S. Günes, H. Neugebauer and N. S. Sariciftci, *Chem. Rev.*, 2007, **107**, 1324–1338.
6 C. Guo, W. Hong, H. Aziz and Y. Li, *Rev. Adv. Sci. Eng.*, 2012, **1**, 200–224.
7 Y. Li, P. Sonar, S. P. Singh, M. S. Soh, M. Van Meurs and J. Tan, *J. Am. Chem. Soc.*, 2011, **133**, 2198–2204.
8 Y. Li, S. P. Singh and P. Sonar, *Adv. Mater.*, 2010, **22**, 4862–4866.
9 J. You, L. Dou, K. Yoshimura, T. Kato, K. Ohya, T. Moriarty, K. Emery, C.-C. Chen, J. Gao, G. Li and Y. Yang, *Nat. Commun.*, 2013, **4**, 1446.
10 G. Li, R. Zhu and Y. Yang, *Nat. Photonics*, 2012, **6**, 153–161.
11 C. Luo, A. K. K. Kyaw, L. A. Perez, S. Patel, M. Wang, B. Grimm, G. C. Bazan, E. J. Kramer and A. J. Heeger, *Nano Lett.*, 2014, **14**, 2764–2771.
12 B. Sun, W. Hong, Z. Yan, H. Aziz and Y. Li, *Adv. Mater.*, 2014, **26**, 2636–2642.
13 X. Guo, M. Baumgarten and K. Müllen, *Prog. Polym. Sci.*, 2013, **38**, 1832–1908.
14 Y. He, W. Hong and Y. Li, *J. Mater. Chem. C*, 2014, **2**, 8651–8661.
15 X. Guo, A. Facchetti and T. J. Marks, *Chem. Rev.*, 2014, **114**, 8943–9021.
16 J. D. Yuen and F. Wudl, *Energy Environ. Sci.*, 2013, **6**, 392–406.
17 I. Kang, H.-J. Yun, D. S. Chung, S.-K. Kwon and Y.-H. Kim, *J. Am. Chem. Soc.*, 2013, **135**, 14896–14899.
18 Y. Li, P. Sonar, L. Murphy and W. Hong, *Energy Environ. Sci.*, 2013, **6**, 1684–1710.
19 R. Kim, P. S. K. Amegadze, I. Kang, H.-J. Yun, Y.-Y. Noh, S.-K. Kwon and Y.-H. Kim, *Adv. Funct. Mater.*, 2013, **23**, 5719–5727.
20 M. Sommer, *J. Mater. Chem. C*, 2014, **2**, 3088–3098.
21 T. Lei, J. H. Dou and J. Pei, *Adv. Mater.*, 2012, **24**, 6457–6461.
22 T. Lei, J.-Y. Wang and J. Pei, *Acc. Chem. Res.*, 2014, **47**, 1117–1126.
23 J. Mei, D. H. Kim, A. L. Ayzner, M. F. Toney and Z. Bao, *J. Am. Chem. Soc.*, 2011, **133**, 20130–20133.
24 W. Hong, C. Guo, Y. Li, Y. Zheng, C. Huang, S. Lu and A. Facchetti, *J. Mater. Chem.*, 2012, **22**, 22282–22289.
25 W. Hong, B. Sun, C. Guo, J. Yuen, Y. Li, S. Lu, C. Huang and A. Facchetti, *Chem. Commun.*, 2013, **49**, 484–486.
26 J.-H. Dou, Y.-Q. Zheng, T. Lei, S.-D. Zhang, Z. Wang, W.-B. Zhang, J.-Y. Wang and J. Pei, *Adv. Funct. Mater.*, 2014, **24**, 6270–6278.
27 J. Y. Back, H. Yu, I. Song, I. Kang, H. Ahn, T. J. Shin, S.-K. Kwon, J. H. Oh and Y.-H. Kim, *Chem. Mater.*, 2015, **27**, 1732–1739.
28 S. Chen, B. Sun, W. Hong, H. Aziz, Y. Meng and Y. Li, *J. Mater. Chem. C*, 2014, **2**, 2183–2190.
29 Z. Yan, B. Sun and Y. Li, *Chem. Commun.*, 2013, **49**, 3790–3792.
30 T. Lei, J.-H. Dou, X.-Y. Cao, J.-Y. Wang and J. Pei, *Adv. Mater.*, 2013, **25**, 6589–6593.
31 Long branched alcohols or alkyl halides with C38–C43 are currently only available from Lyn (Beijing) Science & Technology Co., Ltd.
32 J. Pei, T. Lei and J.-H. Dou, Compound with branching alkyl chains, method for preparing the same, and use thereof in photoelectric device, *US patent*, US2014011973A1, 2014.
33 G. Zhang, P. Li, L. Tang, J. Ma, X. Wang, H. Lu, B. Kang, K. Cho and L. Qiu, *Chem. Commun.*, 2014, **50**, 3180.
34 X. Guo, J. Quinn, Z. Chen, H. Usta, Y. Zheng, Y. Xia, J. W. Hennek, R. P. Ortiz, T. J. Marks and A. Facchetti, *J. Am. Chem. Soc.*, 2013, **135**, 1986–1996.
35 A. Roosjen, J. Šmisterová, C. Driessen, J. T. Anders, A. Wagenaar, D. Hoekstra, R. Hulst and J. B. F. N. Engberts, *Eur. J. Org. Chem.*, 2002, 1271–1277.
36 Y. Li, Monomeric, oligomeric and polymeric semiconductors containing fused rings and their devices, *World patent*, WO2014071524A1, 2014.
37 T. Lei, J.-H. Dou, X.-Y. Cao, J.-Y. Wang and J. Pei, *J. Am. Chem. Soc.*, 2013, **135**, 12168–12171.
38 J. Pommerehne, H. Vestweber, W. Guss, R. F. Mahrt, H. Bässler, M. Porsch, J. Daub, H. Bassler, M. Porsch and J. Daub, *Adv. Mater.*, 1995, **7**, 551–554.
39 W. Hong, C. Guo, B. Sun and Y. Li, *J. Mater. Chem. C*, 2015, **3**, 4464–4470.
40 F. C. Spano, *Acc. Chem. Res.*, 2010, **43**, 429–439.
41 J. Zaumseil and H. Sirringhaus, *Chem. Rev.*, 2007, **107**, 1296–1323.
42 Y. Zhao, Y. Guo and Y. Liu, *Adv. Mater.*, 2013, **25**, 5372–5391.
43 N. S. Sariciftci, *Primary photoexcitations in conjugated polymers: molecular exciton versus semiconductor band model*, World Scientific, 1997.
44 Y. Zhu, R. D. Champion and S. A. Jenekhe, *Macromolecules*, 2006, **39**, 8712–8719.
45 Y. He, C. Guo, B. Sun, J. Quinn and Y. Li, *Chem. Commun.*, 2015, **51**, 8093–8096.
46 M. J. Winokur, D. Spiegel, Y. Kim, S. Hotta and A. J. Heeger, *Synth. Met.*, 1989, **28**, 419–426.
47 H. Sirringhaus, P. J. Brown, R. H. Friend, M. M. Nielsen, K. Bechgaard, B. M. W. Langeveld-Voss, A. J. H. Spiering, R. A. J. Janssen, E. W. Meijer, P. Herwig and D. M. de Leeuw, *Nature*, 1999, **401**, 685–688.